MINERALOGICAL MAGAZINE, MARCH 1978, VOL. 42, PP. 144-6

The crystal structure of hohmannite, $Fe_2(H_2O)_4[(SO_4)_2O].4H_2O$ and its relationship to amarantite, $Fe_2(H_2O)_4[(SO_4)_2O].3H_2O$

F. SCORDARI

Istituto di Mineralogia e Petrografia dell'Università di Bari, Italy

HOHMANNITE is a hydrated sulphate of ferric iron with the formula $Fe_2(SO_4)_2(OH)_2.7H_2O$ (Palache, Berman, and Frondel, 1951).

Figs. 1 and 2 illustrate the structure of hohmannite. The first shows a complex chain of $Fe(O, H_2O)_6$ octahedra and SO_4 tetrahedra, which runs along the *c* axis; the second visualizes the water molecules and an hypothetical hydrogen-bonds system obtained on the basis of electrostatic and geometrical considerations.

Except for the hydroxyl groups, the structure results agree with the composition mentioned above. In fact, according to the hydrogen bonds system shown in fig. 2, no hydroxyl group exists, consequently the chemical formula $Fe_2(H_2O)_4[(SO_4)_2O].4H_2O$ seems more reliable.

In hohmannite there are two $Fe(O, H_2O)_6$ octahedra, two SO_4 tetrahedra, four coordinating and four structural waters crystallographically independent. Both Fe(1) and Fe(2) exibite a distorted octahedral coordination with cation-anion distances ranging from 1·93 to 2·06 Å and 1·87 to 2·10 Å respectively. Fe(1) is surrounded by five oxygens and one water molecule, Fe(2) by three oxygens and three waters. The two SO_4 groups have both three longer and one shorter distances. Two centrosymmetrical pairs of $Fe(O, H_2O)_6$ octahedra and SO_4 tetrahedra are linked together to form a group of composition $[Fe_4(H_2O)_4O_8(SO_4)_4]^{12-}$. These groups polymerize via O(8) to form chains of Fe-O-S linkages along *c*. Coordinating and structural water molecules provide the hydrogen bond system to connect these chains.

Taking into account the linkages between $Fe^{3+}(O, OH, H_2O)_6$ octahedra and SO_4 tetrahedra Süsse (1971) gives a crystal-chemical classification of some natural ferrisulphates. According to this classification hohmannite, like amarantite, belongs to the second type of the three quoted, i.e. infinite chains of Fe-O-S linkages.

Hohmannite, $Fe_2(H_2O)_4[(SO_4)_2O].4H_2O$, is in effect a higher hydrate of amarantite, $Fe_2(H_2O)_4[(SO_4)_2O].3H_2O$, and has been obtained from amarantite by a partial dehydration followed by a successive rehydration (Césbron, 1964). The solution of the structure of hohmannite permits a useful comparison with the structure of amarantite (Süsse, 1968; Giacovazzo and Menchetti, 1969). Both these minerals have the same $P\bar{1}$ space group, comparable reticular parameters, and differ chemically only by the water content. This last difference affects the orientation of the chains' repeat unit $[Fe_4(H_2O)_4O_8(SO_4)_4]^{12-}$ and the hydrogen bond system. In fact owing to the greater number of water molecules in hohmannite, these units under-go some modification, of which the more important is a rotation of about 50°. The consequence of this is the breakage of the hydrogen bond system of amarantite and the building of a new one in hohmannite.

Scharizer (1927) and Césbron (1964) give for hohmannite and amarantite comparable TGA curves, in agreement with the structural results. The only difference in these curves is that hohmannite starts dehydration at normal temperature, amarantite from 60 °C onwards. The structural explanation is that O(17)w forms the weaker hydrogen bonds and, of course, has the higher temperature factor. So this water seems to be the first to be lost by hohmannite in the reaction amarantite $+ 1H_2O \rightleftharpoons$ hohmannite.

The structure of hohmannite accounts for some physical properties, as a higher refractive index compared with amarantite, the elongation on the [001] direction and cleavage on {010}, {1$\bar{1}$0}, and {110} quoted in Dana's System of Mineralogy and on {100} (not quoted).

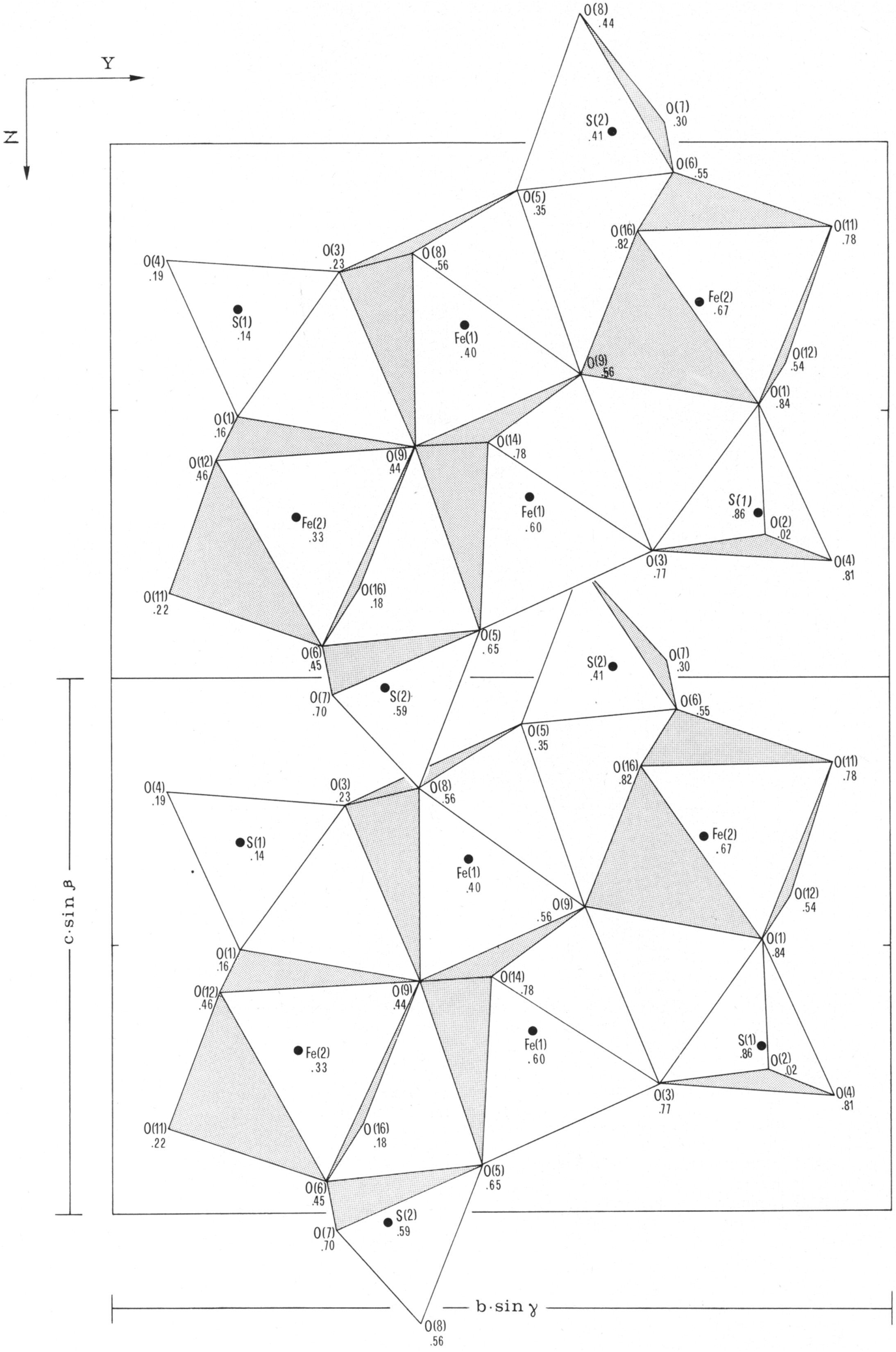

FIG. 1. Chain of Fe–O–S linkages running along the *c*-axis. Next to each atom is given its *x* coordinate.

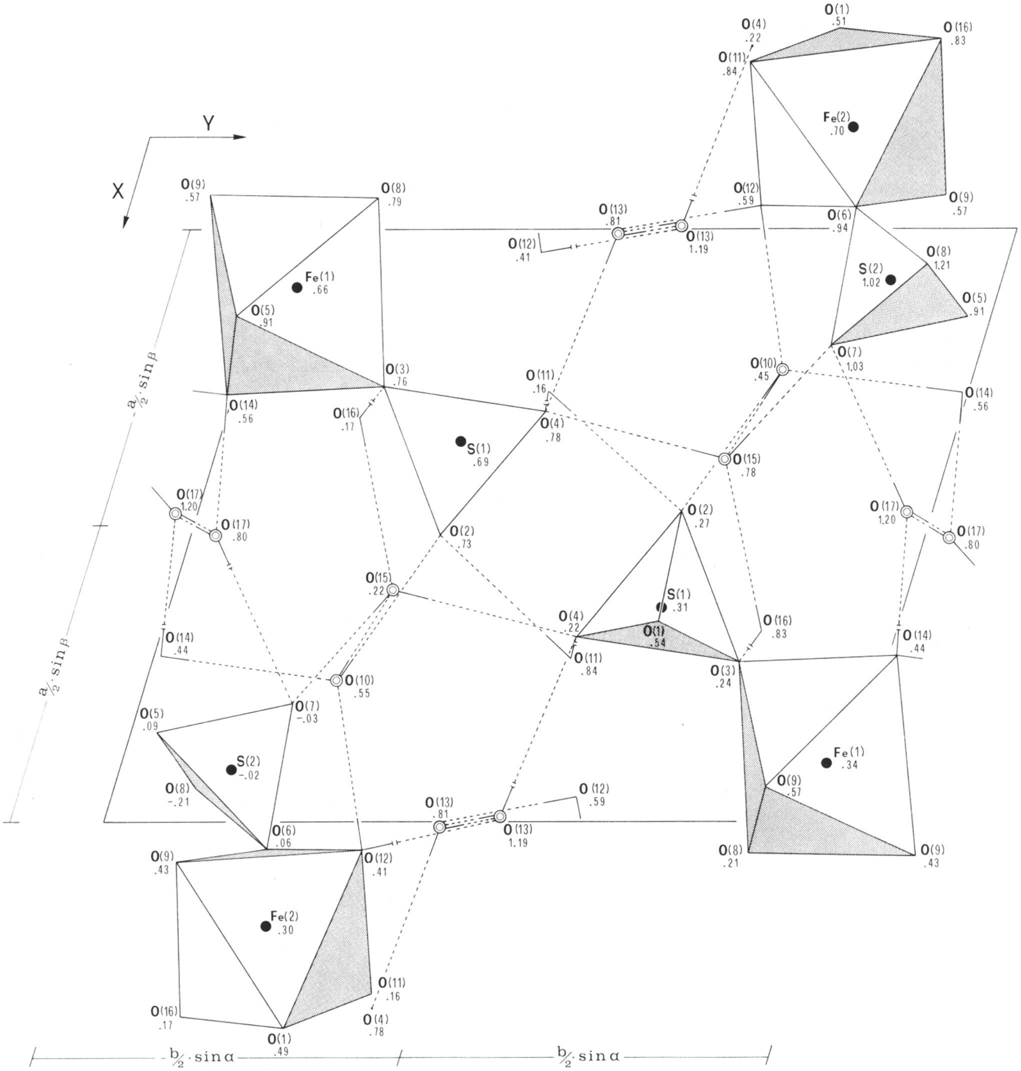

FIG. 2. The crystal structure of hohmannite showing the water molecules and the probable hydrogen-bond system. Next to each atom is given its z coordinate.

REFERENCES

Césbron (F.), 1964. *Bull. Soc. fr. Minéral. Cristallogr.* **87**, 125.

Giacovazzo (C.) and Menchetti (S.), 1969. *Rend. Soc. Ital. Mineral. Petrol.* **25**, 399.

Palache (C.), Berman (H.), and Frondel (C.), 1951. *Dana's System of Mineralogy*, 7th edn., **2**, 456. Wiley, New York.

Scharizer (R.), 1927. *Z. Kristallogr.* **65**, 335.

Süsse (P.), 1968. Ibid. **127**, 261.

—— 1971. *Fortschr. Mineral.* **49**, 119.

[*Manuscript received 25 February 1977; revised 2 June 1977*]

Full text in the Miniprint section, pp. M9–11.

F. Scordari: The structure of hohmannite

M9

THE CRYSTAL STRUCTURE OF HOHMANNITE, $Fe_2(H_2O)_4[SO_4)_2O].4H_2O$ AND ITS RELATIONSHIP TO AMARANTITE, $Fe_2(H_2O)_4[(SO_4)_2O].3H_2O$.

F.Scordari

Istituto di Mineralogia e Petrografia dell'Università di Bari, Italy.

Hohmannite is a hydrated sulphate of ferric iron with the formula $Fe_2(SO_4)_2(OH)_2.7H_2O$ according to Palache, Berman, and Frondel (1951) and to Strunz (1970). The composition of the mineral has been verified by several authors, who give comparable analyses. It has been found associated with other secondary sulphates in desert areas.

Hohmannite was mistaken for amarantite by Frenzel, who first described it in 1887, according to Cesbron (1964). Darapsky (1890) and Rogers (1931) studied as castanite a mineral that Ungemach (1935) showed to be hohmannite. The 'castanite' of Banty (1932) has indices of refraction very near to those given later by the same author for hohmannite (Bandy, 1938). Cesbron (1964) found hohmannite to be triclinic, with a 9.05(2), b 10.88(2), c 7.17(2) Å, α 90°9', β 90°35', γ 106°58', and Z=2. The determination of the crystal structure of hohmannite allows a useful comparison to be made with the structure of amarantite, already determined by Süsse (1968) and by Giacovazzo and Menchetti (1969). The small difference between the structures accounts for some physical analogies that characterize these two minerals.

Esperimental. The crystal employed in this study is from a sample from Sierra Gorda, Chile, kindly supplied by Dr Cesbron. Before starting to measure the intensities it was lacquered to prevent dehydration as much as possible. A small prismatic crystal was investigated by Weissenberg photography to verify the symmetry. According to Cesbron (1964) it is triclinic, and both P1 and $P\bar{1}$ were possible; however, a piezoelectric test showed P1 to be more reliable.

The lattice parameters of hohmannite were refined by the least-squares method applied to 22 accurately indexed reflections from an X-ray powder pattern. Crystal data are: a 9.148(1), b 10.922(1), c 7.183(3) Å, α 90.29(6)°, β 90.79(4)°, γ 107.36(2)°, $\mu_{Mo-K\alpha}$ 25.1 cm^{-1} $\mu R_{max.}$ 0.6, V 684.9 $Å^3$, Z 2, $\rho_{meas.}$ 2.255 $g.cm^{-3}$, $\rho_{calc.}$ 2.250 $g.cm^{-3}$

Intensities were collected by means of a Phillips PW 1100 four-circle automatic diffractometer (Centro di Cristallografia Strutturale del C.N.R., Pavia, Italy) with Mo radiation employing ω-2θ scan technique. The scan rate was 0.04°/sec and the scan range 2°. Within a 2θ range of 50° a total of 2411 reflections were collected, of which 1807 with $I > 3\sigma(I)$ were used in the refinement. The intensities were corrected for Lorentz effect and polarization but not for the absorption effect.

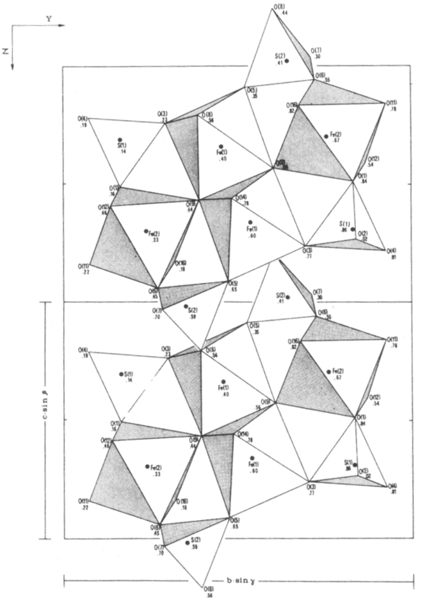

Fig. 1. Chain of Fe-O-S linkages running along the c axis. Next to each atom is given its x coordinate.

TABLE 1. Fractional atomic coordinates, anisotropic temperature factors ($x10^3$), and equivalent temperature factors according to Hamilton (1959). Standard deviations are in parentheses.

Atom	x	y	z	β_{11}	β_{22}	β_{33}	β_{12}	β_{13}	β_{23}	B_H
Fe(1)	0.4022(1)	0.4571(1)	0.3384(1)	4.8(1)	2.2(1)	2.8(1)	0.3(1)	0.5(1)	-0.7(1)	0.9
Fe(2)	0.6693(1)	0.7607(1)	0.3044(1)	5.5(1)	2.3(1)	2.9(2)	0.0(1)	0.9(1)	-0.4(1)	1.0
S(1)	0.1399(2)	0.1742(1)	0.3089(2)	5.6(2)	2.7(1)	4.0(3)	0.1(1)	0.4(2)	-0.9(1)	1.0
S(2)	0.5915(2)	0.3543(1)	0.0194(2)	5.2(2)	2.5(1)	3.0(3)	0.9(1)	0.9(2)	-0.5(1)	0.9
O(1)	0.1645(5)	0.1685(4)	0.5126(6)	7.3(7)	5.5(4)	3.7(9)	-0.9(4)	-0.1(6)	0.0(5)	1.8
O(2)	-0.0193(5)	0.1574(4)	0.2700(6)	6.3(7)	5.2(5)	10.9(10)	0.4(4)	-0.1(6)	-1.4(5)	1.5
O(3)	0.2334(5)	0.3017(4)	0.2431(6)	8.0(6)	3.6(4)	4.2(9)	-0.1(4)	1.1(6)	-0.2(5)	1.5
O(4)	0.1929(5)	0.0750(4)	0.2173(6)	13.0(7)	3.3(5)	8.4(10)	2.4(5)	2.9(6)	-1.7(5)	1.8
O(5)	0.3531(5)	0.5279(4)	0.0900(6)	7.9(6)	4.2(4)	5.5(9)	-0.8(4)	-0.8(6)	0.9(5)	1.6
O(6)	0.5523(5)	0.7270(4)	0.0634(6)	8.5(6)	3.7(4)	4.4(9)	-0.8(4)	0.0(6)	-0.2(5)	1.6
O(7)	0.7045(5)	0.2876(4)	0.0300(6)	11.6(7)	6.7(5)	6.5(10)	5.6(4)	1.1(6)	-0.7(5)	1.9
O(8)	0.5600(5)	0.3901(4)	0.2093(6)	7.7(6)	5.5(4)	2.6(9)	2.7(4)	1.1(6)	-1.6(5)	1.5
O(9)	0.5568(4)	0.6123(4)	0.4259(5)	5.2(5)	2.3(4)	2.8(8)	0.0(4)	0.4(5)	-0.6(4)	0.9
O(10)w	0.7442(7)	0.2428(6)	0.4473(8)	13.8(9)	7.4(6)	23.0(13)	3.2(6)	6.4(9)	-0.8(7)	2.5
O(11)w	0.7797(5)	0.9303(4)	0.1632(6)	11.6(6)	4.2(4)	3.3(9)	-1.1(4)	1.3(6)	0.1(5)	2.0
O(12)w	0.5379(5)	0.8648(4)	0.4061(6)	10.4(7)	4.2(5)	10.1(10)	3.2(5)	3.5(6)	0.1(5)	1.6
O(13)w	0.4877(6)	0.0406(5)	0.1892(8)	15.3(9)	8.0(6)	14.4(12)	6.1(6)	3.4(8)	2.5(7)	2.5
O(14)w	0.2234(5)	0.5126(4)	0.4426(6)	5.7(7)	5.8(5)	12.1(9)	2.4(4)	1.4(6)	-2.4(5)	1.4
O(15)w	0.1128(6)	0.8051(5)	0.2167(7)	9.7(8)	6.4(6)	19.3(12)	2.6(5)	3.6(8)	-2.1(6)	1.9
O(16)w	0.8182(5)	0.6790(4)	0.1751(6)	8.5(7)	5.9(5)	9.9(10)	2.3(5)	1.6(6)	-2.8(5)	1.7
O(17)w	0.9839(8)	0.4732(7)	0.2052(10)	12.3(12)	13.5(9)	32.1(18)	3.0(8)	-4.4(12)	-1.0(10)	3.3

Solution of the structure and refinement. The space group P1 was initially chosen and later confirmed by the crystal structure success. Some preliminary considerations were useful: Hohmannite and amarantite are two very closely related minerals, and similariities such as chemical formulae, lattice constants, spacr groups, and thermal data seemed to indicate that the structural units of tetrahedra and octahedra present in amarantite were probably also present in hohmannite. The positions of two crystallographically independent iron and two sulphur atoms were determined with the aid of three-dimensional Patterson syntheses. Subsequent structure-factor calculations and Fourier syntheses led to the determination of the positions of all 21 independent non-hydrogen atoms.

The refinement of the parameters was carried out by a full-matrix least-squares method using the program ORFLS (Busing, Martin, and Levy, (1962). The atomic-scattering curves were prepared from the values given in the International Tables (1962). All reflections were given unit weight. At the end of the refinement, including scale factor, positional parameters, and thermal factors, the R value was 0.075 in the isotropic temperature-factor mode, and 0.039 in the anisotropic one

Table II. Bond distances involving Fe-O and S-O atoms in hohmannite and amarantite (Süsse, 1968), with their standard deviations

	Hohmannite	Amarantite		Hohmannite	Amarantite
Fe(1)-O(3)	2.032(4)Å	2.042(6)Å	Fe(2)-O(16)w	2.066(5)Å	2.069(6)Å
-O(5)	2.045(4)	2.085(6)			
-O(8)	2.034(4)	2.045(6)	S(1)-O(1)	1.481(5)	1.496(6)
-O(9)	1.949(4)	1.923(6)	-O(2)	1.436(5)	1.456(6)
-O($\bar{9}$)	1.935(4)	1.969(6)	-O(3)	1.483(4)	1.495(6)
-O(14)w	2.056(5)	2.091(6)	-O(4)	1.469(5)	1.456(6)
Fe(2)-O(1)	1.967(4)	1.986(6)	S(2)-O(5)	1.470(5)	1.489(6)
-O(6)	1.996(4)	2.028(6)	-O(6)	1.466(4)	1.495(6)
-O(9)	1.870(4)	1.892(6)	-O(7)	1.433(5)	1.439(6)
-O(11)w	2.100(5)	2.074(6)	-O(8)	1.473(4)	1.489(6)
-O(12)w	2.025(5)	2.052(6)			

w: Oxygen of water molecules

Atomic coordinates and temperature factors are listed in Table I. A table containing observed and calculated structure factors is deposited in the library of the Dept.of Mineralogy, British Museum (Natural History), from which copies may be purchased.

M10

Structure analysis. Schematic and partial views of the structure of hohmannite are shown in figs. 1 and 2. The first represents a structural unit that is the skeleton of the structure, while the second visualizes the water molecules and their function in connecting similar units like that illustrated in fig.1. For ease of comparison, the sketches and designations accepted for hohmannite conform with those used by Süsse (1968) for amarantite.

The two crystallographically independent Fe atoms are surrounded octahedrally by oxygen atoms. Some of these are water molecules, which in the Tables are indicated by w. The individual ranges of Fe(1)-O and Fe(2)-O distances lie between 1.92 and 2.06 Å and between 1.87 and 2.10 Å respectively. Both ranges agree with those found in amarantite, which are 1.92 to 2.09 Å for Fe(1)-O and 1.89 to 2.07 Å for Fe(2)-O. For fuller details see Tables II and III, in which there is a systematic comparison of the distances and angles of equivalent polyhedra in the two minerals.

In hohmannite there are two SO_4 groups symmetrically unrelated. However, both have three longer and one shorter distance, whereas in amarantite the S(1) tetrahedron has two longer and two shorter distances (Table II). These differences can be partly explained on the basis of the proposed hydrogen-bond system for hohmannite (fig.2). In fact, O(4) appears to be linked by hydrogen bonds to three water molecules in hohmannite, in amarantite only to two (fig.6). Another difference between the structures of the two minerals concerns the angles and the cation-anion distances as a whole; the modifications involving angles and distances are directly connected with the two additional water molecules in the unit cell of hohmannite. As regards the angles we may note that those related to Fe atoms are more affected than those related to S atoms (Table III). The weighted mean values of the cation-anion distances, $\overline{\text{Fe(1)-O}}$ 2.007(4), $\overline{\text{Fe(2)-O}}$ 1.997(5), $\overline{\text{S(1)-O}}$ 1.468(5), and $\overline{\text{S(2)-O}}$ 1.462(5) in hohmannite, are all shorter than the corresponding distances in amarantite, $\overline{\text{Fe(1)-O}}$ 2.026(6), $\overline{\text{Fe(2)-O}}$ 2.017(6), $\overline{\text{S(1)-O}}$ and $\overline{\text{S(2)-O}}$ 1.478(6) Å. This small but significant difference (with the exception of S(1)-O owing to the S(1)-O(4) distance) can be ascribed to the higher density of hohmannite (2.25 $g.cm^{-3}$) compared with that of amarantite (2.14 $g.cm^{-3}$). Also an analysis of the atomic density carried out around Fe and S polyhedra shows a greater crowding of first neighbour oxygen atoms in hohmannite.

As in amarantite two centrosymmetrical paies of octahedra and tetrahedra are connected to form a group of composition $Fe_4(H_2O)_4O_8(SO_4)_4$ as shown in fig.3. Such groups sharing O(8) polymerize to form chains of Fe-O-S linkages along c. The connections between these chains form a complex system of hydrogen bonds. This system could not be resolved directly by a difference Fourier synthesis but only by the agreement of the electrostatic valency balance and geometric criteria (Tables IV, V, and VI); moreover, the scheme illustrated in fig.4 agrees with the behaviour of the hydrogen-bond system in amarantite (fig.5) - i.e. the water molecules linked to Fe^{3+} are only of Evans's A-type (Evans, 1964). From fig.4 one can see that O(17)-O(17) and O(13)-O(13) are two pairs of water molecules linked to each other by a double hydrogen bond. This is because from the analysis of O-O distances less tahn 3.20 Å (Table IV), coupled to the electrostatic requirements (Table VI), only two of the four possibile pairs seem available for

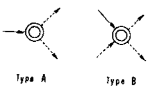

Fig.4. Sketches of two possible types of water molecules (double circles) linked to a trivalent cation (modified from Evans, 1964). In the structure of hohmannite only the A-type is present, as in the structure of amarantite. The unbroken arrows indicate the Fe-O bonds, the broken ones the H-O bonds.

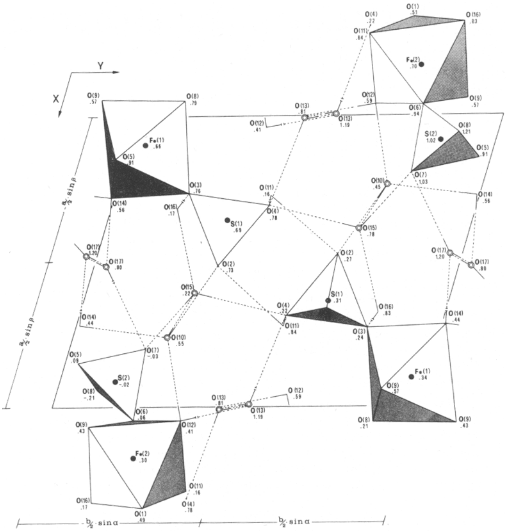

Fig.2. The crystal structure of hohmannite showing the water molecules and the probable hydrogen-bond system. Next to each atom is given its z coordinate.

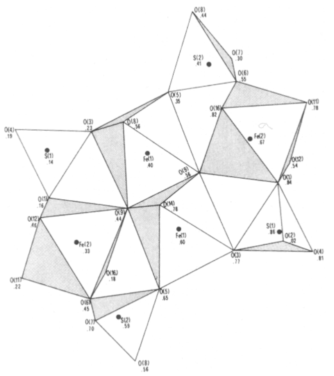

Fig.3. The group of composition $Fe_4(H_2O)_4O_8(SO_4)_4$ found in hohmannite.

Table III. O-S-O and O-Fe-O bond angles with standard deviations in parentheses. The values of hohmannite (this study) are compared with those of amarantite (Süsse, 1968).

Atoms involved	Angles (this study)	Angles (Süsse)	Atoms involved	Angles (this study)	Angles (Süsse)
O(3)-Fe(1)-O(5)	80.6(2)°	84.9(2)°	O(9)-Fe(2)-O(16)w	96.1(2)°	86.3(2)°
O(3)-Fe(1)-O(8)	89.7(2)	89.8(2)	O(9)-Fe(2)-O(1)	100.8(2)	98.9(2)
O(3)-Fe(1)-O(9)	176.7(2)	169.8(2)	O(11)w-Fe(2)-O(12)w	84.0(2)	92.4(2)
O(3)-Fe(1)-O(14)w	83.9(2)	80.5(2)	O(11)w-Fe(2)-O(16)w	87.1(2)	88.5(2)
O(3)-Fe(1)-O($\overline{9}$)	98.2(2)	95.2(2)	O(11)w-Fe(2)-O(1)	82.3(2)	85.9(2)
O(5)-Fe(1)-O(8)	89.5(2)	82.8(2)	O(12)w-Fe(2)-O(16)w	171.1(2)	175.3(2)
O(5)-Fe(1)-O(9)	97.1(2)	97.5(2)	O(12)w-Fe(2)-O(1)	93.3(2)	85.2(2)
O(5)-Fe(1)-O(14)w	86.0(2)	89.8(2)	O(16)w-Fe(2)-O(1)	86.4(2)	93.3(2)
O(5)-Fe(1)-O($\overline{9}$)	178.5(2)	172.1(2)			
O(8)-Fe(1)-O(9)	92.7(2)	100.3(2)	O(1)-S(1)-O(2)	109.5(3)	110.7(3)
O(8)-Fe(1)-O(14)w	172.6(2)	168.3(2)	O(1)-S(1)-O(3)	108.3(3)	107.5(3)
O(8)-Fe(1)-O($\overline{9}$)	91.4(2)	89.3(2)	O(1)-S(1)-O(4)	108.9(3)	109.2(3)
O(9)-Fe(1)-O(14)w	93.6(2)	89.6(2)	O(2)-S(1)-O(3)	109.8(3)	109.2(3)
O(9)-Fe(1)-O($\overline{9}$)	84.0(2)	83.7(2)	O(2)-S(1)-O(4)	111.7(3)	112.7(3)
O(14)w-Fe(1)-O($\overline{9}$)	93.0(2)	98.0(2)	O(3)-S(1)-O(4)	108.6(3)	107.3(3)
O(6)-Fe(2)-O(9)	97.2(2)	94.4(2)	O(7)-S(2)-O(8)	108.7(3)	111.0(3)
O(6)-Fe(2)-O(11)w	80.1(2)	82.6(2)	O(7)-S(2)-O(5)	111.0(3)	110.8(3)
O(6)-Fe(2)-O(12)w	92.5(2)	84.3(2)	O(7)-S(2)-O(6)	111.3(3)	110.1(3)
O(6)-Fe(2)-O(16)w	85.1(2)	96.5(2)	O(8)-S(2)-O(5)	108.4(3)	109.1(3)
O(6)-Fe(2)-O(1)	160.8(2)	164.0(2)	O(8)-S(2)-O(6)	108.1(2)	107.1(3)
O(9)-Fe(2)-O(11)w	175.6(2)	169.4(2)	O(5)-S(2)-O(6)	109.3(2)	108.7(3)
O(9)-Fe(2)-O(12)w	92.7(2)	91.8(2)			

TABLE IV. Ow - O distances less than 3.20Å related to oxygen atoms not belonging to the same polyhedron. The asterisk indicates atoms in a different unit cell.

O(10)w-O($\overline{2}$)	2.905(8) Å	O(13)w-O(4)	2.841(7) Å
-O(7)	3.074(8)	-O(7)	3.069(7)
-O(8)	3.149(7)	-O($\overline{13}$)w	2.887(11)
-O($\overline{12}$)w	2.725(7)	O(14)w-O*(17)w	2.687(9)
-O($\overline{14}$)w	2.711(7)	O(15)w-O*(4)	2.817(7)
-O($\overline{15}$)w	2.853(8)	-O*(16)w	2.647(7)
O(11)w-O*(2)	2.710(7)	-O(7)	2.834(7)
-O(6)	2.637(6)	O(16)w-O(17)w	3.070(9)
-O($\overline{1}$)	2.677(7)	-O(1)	2.762(7)
-O($\overline{4}$)	2.750(6)	-O($\overline{3}$)	3.052(6)
O(12)w -O(6)	2.904(6)	-O($\overline{5}$)	2.991(7)
-O*(13)w	2.619(7)	O(17)w-O(7)	3.003(9)
-O($\overline{13}$)w	3.116(7)	-O(17)w	3.010(14)
-O($\overline{1}$)	2.904(6)		

a hydrogen bond: O(17)-O(17) and O(17-O(7). If we suppose that there is also centrosymmetry for the hydrogen bonds, a double hydrogen bond between O(17) and O(17) is the result. From this we derive that O(13) is also stabilized by a double hydrogen bond. The electrostatic valency balance was computed taking into account the individual bond-strength bond-length parameters given by Brown and Shannon (1973). The bond-strengths of O-H...O bonds are derived from the curve of bond valences proposed by Brown and Shannon and further discussed by Donnay and Donnay (1973).

The other two structural water molecules - O(10)w and O(15)w - are surrounded tetrahedrally by four oxygens with bond angles ranging from 84° to 138° and O-O distances from 2.65 to 2.90 Å. According to the system of hydrogen bonds illustrated in fig.2, no hydroxyl groups exist in the structure. In agreement with the chemical composition, the structure suggests eight water molecules, O(10) to O(17), and nine oxygen atoms, O(1) to O(9). In this case the formula $Fe_2(SO_4)_2(OH)_2.7H_2O$ usually quoted for hohmannite seems incorrect, and in the light of the structure determination $Fe_2(H_2O)_4[(SO_4)_2O].4H_2O$ must be preferred.

Relationships between hohmannite and amarantite and conclusions. Hohmannite represents a higher hydrate of amarantite, and has been obtained by a partial dehydration and successive rehydration of amarantite (Cesbron, 1964). The solution of the crystal structure of hohmannite shows the adaptability of the network of amarantite to the admission of two extra water molecules. These minerals are both triclinic with space group P$\overline{1}$; this is because both structures are based on the polymerization of centrosymmetrical groups with composition $Fe_4(H_2O)_4O_8(SO_4)_4$ (fig.3). From a comparison of figs. 2 and 6 one can locate the two new structural water molecules in the network of hohmannite when amarantite hydrates. In fact, in spite of some modifications occurring in the rearrangement of the crystal structure it is still possible to recognize in O(17) the structural water involved in the reaction amarantite + H_2O hohmannite. The entrance of water into the structure of amarantite has two main effects: the first involves the $Fe_4(H_2O)_4O_8(SO_4)_4$ group and the second the hydrogen-bond system.

The groups just mentioned are forced in hohmannite to adopt changes in configuration, of which the more important is a rotation of the polymerized groups by about 50°. The components of this rotation are about 20° and 45° in the crystallographic planes (100) and (001) respectively (compare figs. 1 and 5, also 2 and 6). Of course the reorientation of the groups based on Fe-O-S linkages involves the disruption of the old hydrogen-bond system and the building of a more suitable one (figs. 2 and 6). The crystal structures of amarantite and hohmannite account for the similar dehydration curves found by Scharizer (1927) and by Cesbron (1964). Hohmannite starts dehydrating at a lower temperature than amarantite; the longer O-O distances found for O(17)w and the higher temperature factor for these water molecules (Table I) agree with this result.

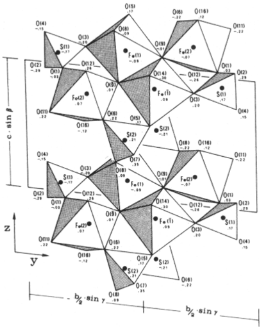

Fig. 5. Chain of octahedra and tetrahedra parallel to the c axis in amarantite. Next to each atom is given its x coordinate.

Table V. Angles involving the ligand water oxygens in agreement with the proton-donors/proton-acceptors scheme proposed in fig.2. The asterisk indicates atoms in a different unit cell.

O($\overline{14}$)w-O(10)w-O($\overline{12}$)w	= 97.0(2)°	O($\overline{10}$)w-O(14)w-O*(17)w	= 100.3(2)°
O($\overline{14}$)w-O(10)w-O($\overline{2}$)	= 124.8(2)	O(7)-O(15)w-O($\overline{10}$)w	= 96.5(2)
O($\overline{14}$)w-O(10)w-O($\overline{15}$)w	= 91.1(2)	O(7)-O(15)w-O*(16)w	= 111.7(2)
O($\overline{12}$)w-O(10)w-O($\overline{2}$)	= 137.8(2)	O(7)-O(15)w-O*(4)	= 111.8(2)
O($\overline{12}$)w-O(10)w-O($\overline{15}$)w	= 90.6(2)	O($\overline{10}$)w-O(15)w-O*(16)w	= 115.9(2)
O($\overline{15}$)w-O(10)w-O($\overline{2}$)	= 83.7(2)	O($\overline{10}$)w-O(15)w-O*(4)	= 102.0(2)
O*(2)-O(11)w-O($\overline{4}$)	= 104.2(2)	O*(4)-O(15)w-O*(16)w	= 116.7(2)
O*(13)w-O(12)w-O($\overline{10}$)w	= 101.8(2)	O*(15)w-O(16)w-O($\overline{3}$)	= 102.3(2)
O($\overline{13}$)w-O(13)w-O(4)	= 106.5(3)	O*(14)w-O(17)w-O($\overline{17}$)w	= 123.5(4)
O*(12)w-O(13)w-O(4)	= 115.3(2)	O($\overline{17}$)w-O(17)w-O(7)	= 75.5(3)

Table VI. Electrostatic valency balance in hohmannite.

Atom	Fe	S	...H	Sums	Atom	Fe	H--	...H	Sums
O(1)	0.54†	1.45‡	-	1.99	O(10)w	-	0.83 0.84	0.20 0.21	2.08
O(2)	-	1.61‡	0.16 0.21	2.04	O(11)w	0.38†	0.79 0.81	-	1.98
O(3)	0.46*	1.44‡	0.14	2.04	O(12)w	0.47†	0.80 0.76	-	2.03
O(4)	-	1.50‡	0.19 0.18 0.18	2.05	O(13)w	-	0.82 0.83	0.24 0.17	2.06
O(5)	0.46*	1.465‖	-	1.925	O(14)w	0.43*	0.79 0.78	-	2.00
O(6)	0.50†	1.465‖	-	1.965	O(15)w	-	0.82 0.82	0.23 0.17	2.04
O(7)	-	1.60‖	0.18 0.15	1.93	O(16)w	-	0.86 0.77	-	2.04
O(8)	0.46*	1.47‖	-	1.93	O(17)w	-	0.85 0.85	0.22 0.15	2.07
O(9)	0.61* 0.58† 0.70†	-	-	1.89					
Sums	-	12.00	-	-		6.00	13.02	2.98	34.00

* Fe(1); † Fe(2); ‡ S(1); ‖ S(2). The hydrogen atoms are, or course, members of O(10)w to O(17)w.

Hohmannite loses its structural water below 100°C (as does amarantite). According to Cesbron, in the range 95 to 143°C the TGA curve of hohmannite shows a plateau that corresponds to metahohmannite, $Fe_2(SO_4)_2(OH)_2.3H_2O$. In agreement with this result it seems reasonable to suppose that in hohmannite too there is a group of composition $Fe_4(H_2O)_4O_8(SO_4)_4$. Consequently metahohmannite should represent the lower boundary of the series hohmannite-amarantite-metahohmannite, in which all the structural water is lost.

The cyrstal structure of hohmannite accounts for the elongation in the [001] direction, for the cleavage (010), (110), and (1$\overline{1}$0) quoted in Dana's System (Palache, Berman, and Frondel, 1951), and for (100) not quoted. It accounts too for the higher refractive indices than those of amatantite.

Acknowledgements. We thank Dr F.Cesbron for supplying the crystals. This paper was supported by C.N.R. Contract no. 75.1066.05.115.4593.

REFERENCES

Bandy (M.C.), 1932. Am.Mineral.17, 534.
(1938). Ibid. 23, 735.
Brown (I.D.) and Shannon (R.D.), 1973. Acta Cwystallogr. A29, 266
Busing (W.R.), Martin (K.O.), and Levy (H.A.), 1962. ORFLS Report ORNL-TM305, Oak Ridge Natl.Lab., Oak Ridge, Tennessee.
Cesbron (F.), 1964. Bull.Soc.fr.Minéral.Crystallogr.87, 125
International Tables for X-ray Crystallography (1962), 3. Kynoch Press.
Darapsky (L.), 1890. Quoted by F.Cesbron, 1964.
Donnay (G.) and Donnay (J.D.H.), 1973. Acta Crystallogr. B29, 1417.
Evans (R.C.), 1964. Crystal Chemistry, 2nd edn. Cambridge Univ.Press.
Giacovazzo (C.) and Menchetti (S.), 1969. Rend.Soc.Ital.Mineral.Petrol. 25, 399.
Rogers (A.F.), 1931. [Am.Mineral.16, 396], quoted by F.Cesbron, 1964.
Scharitzer (R.), 1927. Z.Kristallogr.65, 335.
Strunz (H.), 1970. Mineral.Tabellen, 5th edn. Leipzig, Akad.Verlag.
Süsse (P.), 1968. Z.Kristallogr.127, 261.
Ungemach (H.), 1935. [Bull.Soc.fr.Minéral.Crystallogr.58, 97], quoted by F.Cesbron, 1964.

[Manuscript received 25 February 1977]

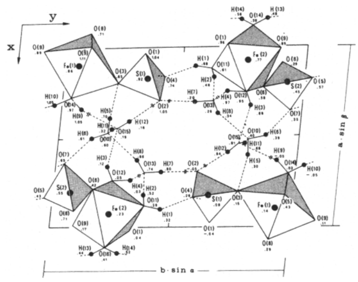

Fig. 6. The crystal structure of amarantite which shows up the water molecules and the related hydrogen-bond system. Next to each atom is given its z coordinate.

TABLE I. Representative electron microprobe analyses of olivines, orthopyroxenes and clinopyroxenes, Wairere Serpentinite, New Zealand.

	1	2	3	4	5	6	7	8	9	10	11	12	13	14	15	16	17
SiO_2	39.7	51.8	51.1	50.1	51.8	51.9	51.3	51.7	52.2	50.0	51.6	49.7	49.1	50.4	52.9	52.4	52.78
TiO_2	-	-	0.08	0.09	1.24	1.36	1.59	1.42	0.87	1.40	1.67	2.55	1.40	2.44	0.04	0.18	0.24
Al_2O_3	-	2.45	1.62	1.34	3.89	4.24	3.82	2.81	1.97	3.48	3.55	3.29	3.06	2.66	1.57	2.22	2.43
Cr_2O_3	-	-	-	-	0.18	0.20	0.21	0.21	0.21	0.21	0.22	0.21	0.17	0.20	0.21	-	0.95
FeO*	20.4	9.4	13.8	22.5	5.74	5.82	6.28	7.52	7.16	9.64	7.84	10.7	10.5	11.2	7.23	9.40	2.31
MnO	0.18	0.27	0.13	0.29	-	-	0.09	0.01	0.07	0.05	0.07	-	0.07	-	0.21	0.21	0.32
MgO	39.4	35.8	30.6	23.2	17.0	16.9	16.2	16.7	17.6	16.4	16.1	15.1	18.1	15.9	15.7	13.5	18.75
CaO	-	0.58	0.55	0.79	20.0	20.0	19.6	19.1	19.1	18.9	18.8	17.9	18.4	17.8	21.2	22.0	20.86
Na_2O	-	0.13	0.24	0.19	0.02	0.07	0.20	0.19	0.20	0.21	0.19	0.20	-	0.22	0.08	0.22	0.60
K_2O		-	-	-	-	-	0.02	0.02	0.01	-	-	-	-	-	-	-	-
Total	99.68	100.43	98.12	98.50	99.87	100.48	99.31	99.68	99.39	100.29	100.04	99.65	100.80	100.82	99.14	100.13	99.24
Structural formula on a basis of 4(ol), 6(opx and cpx) oxygen atoms																	
Si	1.02	1.83	1.88	1.91	1.89	1.89	1.89	1.91	1.93	1.86	1.90	1.86	1.83	1.87	1.97	1.95	1.93
Al	-	0.10	0.07	0.06	0.17	0.18	0.17	0.12	0.09	0.15	0.15	0.14	0.13	0.12	0.07	0.10	0.11
Ti	-	-	<0.01	<0.01	0.03	0.04	0.04	0.03	0.02	0.04	0.05	0.07	0.04	0.07	-	0.01	0.01
Cr	-	-	-	-	0.01	0.01	0.01	0.01	0.01	0.01	0.01	0.01	0.01	0.01	0.01	-	0.03
Fe^{2*}	0.44	0.28	0.42	0.71	0.18	0.18	0.19	0.23	0.22	0.30	0.24	0.34	0.33	0.35	0.23	0.29	0.07
Mn	<0.01	0.01	<0.01	0.01	-	-	0.01	-	-	-	0.00	-	-	-	0.01	0.01	0.01
Mg	1.51	1.88	1.68	1.32	0.93	0.92	0.89	0.92	0.97	0.91	0.88	0.84	1.00	0.88	0.87	0.75	1.02
Ca	-	0.02	0.02	0.03	0.78	0.78	0.78	0.76	0.76	0.75	0.74	0.72	0.73	0.71	0.84	0.88	0.82
Na	-	0.01	0.02	0.01	-	-	0.01	0.01	0.01	0.02	0.01	0.02	-	0.02	0.01	0.02	0.04
Atomic percent																	
Ca	-	1.0	1.0	1.5	41.5	41.6	41.5	39.6	38.8	38.3	39.7	37.9	35.5	36.6	43.4	45.6	42.6
Mg	77.3	86.0	78.9	63.5	49.1	48.9	47.7	48.2	49.7	46.3	47.3	44.4	48.6	45.5	44.7	38.9	53.2
Fe+Mn	22.7	13.0	20.1	35.0	9.3	9.3	10.8	12.2	11.5	15.4	13.0	17.7	15.9	17.9	11.9	15.5	4.2

1	Relic olivine in highly serpentinised harzburgite, 24725
2	Relic orthopyroxene in highly serpentinised harzburgite, 23449
3,4	Orthopyroxenes, adjacent to hornblende-bearing rodingite vein, 24725 (all such orthopyroxenes yielded low totals)
5,6	Clinopyroxenes, fine-grained rodingite, 23438
7,8,9	" , coarse " " , 23443
10,11	" , " " " , 23444
12	" , from prehnite-pectolite zone, 23434
13	" , altered gabbro, 23444
14	" , " " , 23448
15	" , pyroxene-bearing rodingite vein, 24723
16	" , hornblende-bearing rodingite vein, 24725
17	Relic clinopyroxene in highly serpentinised harzburgite, 23449.
*	Total iron as FeO.

Lensoid bodies

Hornblende gabbro dyke The centre of this body is an unaltered, hard, black, fine-grained rock cut by minor serpentine veins (24720), and shows an aplitic, subophitic texture composed of 60% fine-grained sub-parallel labradorite laths and 40% fine-grained green hornblende, with rare, 2 mm, plagioclase phenocrysts. Accessories include scattered interstitial apatite needles, minor granular magnetite and orange-pink biotite flakes which are aligned, with the plagioclase, parallel to the contact. Plagioclase phenocrysts exhibit normal zoning, with minor sericitization and prehnitization occurring in the more calcic cores, and, in places, poikilitically enclose hornblende and biotite grains. Colourless titanite veinlets, containing rare large euhedral grains, cut the rock and, in one place, partially replace labradorite.

Near the contact, with a 2-3 cm zone of chloritised serpentinite, the hornblende gabbro is altered to a very fine-grained, hard, light grey-brown rodingite (24719) which consists of fine, granular, brown hydrogarnet and colourless chlorite, accessory magnetite and flakes of biotite, concentrated in small elongated red patches parallel to the contact. A dark grey transitional zone, with sharp boundaries and composed of prehnitized plagioclase, fine-grained hornblende, magnetite, biotite and a low birefringent, colourless chlorite occurs between the dyke centre and the marginal rodingite.

Chrysotile veins cut the dyke perpendicular to the contact and have small reaction zones around them containing brown hydrogarnet pseudomorphous after plagioclase.

The rodingite dyke consists of hard, white, rock composed of fine-grained dark-brown, hydrogarnet with local intergranular serpentine. In places the hydrogarnet encloses large clinochlore fragments and partially chloritized clinopyroxene. Some chlorite fragments contain small blebs of garnet. Rare native copper is concentrated along small green chlorite veins (24721). The contact with chloritized serpentinite in 24722 is brecciated with angular fragmented grains of bastite and hydrogarnet set in a groundmass of granular green chlorite. In 24721 the contact with unsheared, mesh-textured serpentinite was sharp and separated from the rodingite by 2 mm of recrystallised serpentinite.

TABLE II. Representative microprobe analyses of amphiboles, Wairere Serpentinite

	18	19	20	21	22	23
SiO_2	51.3	51.6	49.5	48.5	48.9	49.8
TiO_2	0.50	0.41	0.56	0.48	0.68	0.42
Al_2O_3	4.63	4.91	5.52	5.86	5.00	6.38
FeO*	15.9	15.9	11.2	11.1	15.8	15.6
MnO	0.31	0.24	0.10	0.10	0.28	0.30
MgO	13.9	13.8	17.3	16.8	13.6	13.2
CaO	11.2	11.2	11.6	11.8	11.5	12.0
Na_2O	0.63	0.70	1.15	1.11	0.72	0.62
K_2O	0.19	0.16	0.12	0.11	0.18	0.16
Total	98.56	98.92	97.05	95.86	96.66	98.48
†Si	7.44	7.46	7.13	7.08	7.24	7.22
Al^{iv}	0.56	0.54	0.87	0.93	0.76	0.78
Al^{vi}	0.23	0.29	0.07	0.08	0.11	0.31
Ti	0.05	0.04	0.06	0.05	0.08	0.05
†Fe^3	0.14	0.15	1.26	0.81	0.77	0.55
†Fe^2	1.79	1.78	0.09	0.54	1.19	1.34
Mn	0.04	0.03	0.01	0.01	0.04	0.04
Mg	3.01	2.98	3.72	3.65	3.00	2.85
Ca	1.74	1.73	1.79	1.84	1.82	1.86
Na	0.18	0.20	0.32	0.31	0.21	0.17
K	0.04	0.03	0.02	0.02	0.03	0.03
‡Si	7.30	7.31	7.03	6.99	7.14	7.15
Al^{iv}	0.70	0.69	0.92	1.00	0.80	0.78
Al^{vi}	0.07	0.13	-	-	-	0.30
Ti	0.05	0.04	0.06	0.05	0.07	0.05
‡Fe^3	0.52	0.78	0.75	0.87	0.85	0.46
‡Fe^2	1.37	1.10	0.57	0.47	1.08	1.41
Mn	0.04	0.03	0.01	0.01	0.04	0.04
Mg	2.95	2.92	3.66	3.61	2.96	2.82
Ca	1.71	1.70	1.76	1.82	1.80	1.85
Na	0.17	0.23	0.32	0.31	0.20	0.17
K	0.03	0.03	0.02	0.03	0.03	0.03

18,19	Actinolitic hornblendes, hornblende gabbro dyke, 24720.
20,21	Magnesio-hornblendes, rodingite vein, 24725.
22	Magnesio-hornblende, altered gabbro pod, 24712.
23	Magnesio-hornblende, altered gabbro pod, 24714.

† structural formula calculated on a basis of 15 cations excluding Na and K. Fe^{3+} is a minimum value consistent with stoichiometry.

‡ structural formula calculated on a basis of 13 cations excluding Ca, Na and K. Fe^{3+} is a maximum value consistent with stoichiometry.

TABLE III. Representative microprobe analyses of biotite and metasomatic chlorites, Wairere Serpentinite

	24	25	26	27	28	29	30	31	32	33	34	35
SiO_2	32.1	31.7	32.8	32.1	32.1	31.7	31.8	35.8	35.8	35.5	25.9	37.3
TiO_2	0.12	0.13	0.10	0.11	0.11	0.09	0.11	0.02	0.03	0.06	0.17	1.93
Al_2O_3	15.1	16.6	14.8	13.8	13.2	17.2	15.6	13.5	12.3	14.7	21.7	15.8
Cr_2O_3	0.03	0.05	0.05	0.09	0.02	0.05	0.07	0.07	0.04	-	0.03	-
FeO*	30.3	30.3	30.5	31.6	33.0	27.0	29.0	5.03	6.56	14.9	28.2	21.9
MnO	0.18	0.18	0.17	0.16	0.17	0.17	0.20	0.12	0.12	0.16	0.11	0.06
MgO	10.4	11.1	10.9	12.8	12.0	14.2	13.3	30.5	29.8	22.6	13.3	11.1
CaO	0.52	0.51	0.51	0.30	0.31	0.33	0.31	0.32	-	0.41	0.30	0.57
Na_2O	0.03	0.03	0.02	-	0.04	-	-	0.06	0.08	0.06	-	0.38
K_2O	-	-	-	-	-	-	-	-	-	-	-	7.66
Total	88.78	90.60	89.85	90.96	90.95	90.74	90.39	85.42	84.73	88.39	89.71	96.70
Structural formulae calculated on a basis of 28(chlorite) and 22(biotite) oxygens												
Si	6.77	6.55	6.83	6.67	6.72	6.42	6.55	6.88	6.98	6.91	5.40	5.61
Al^{iv}	1.23	1.45	1.17	1.33	1.28	1.58	1.45	1.12	1.02	1.09	2.60	2.39
Al^{vi}	2.55	2.59	2.47	2.04	1.98	2.53	2.33	1.94	<1.81	2.28	2.73	0.41
Ti	0.02	0.02	0.02	0.02	0.02	0.01	0.02	-	0.01	0.01	0.03	0.22
Cr	0.01	0.01	0.01	0.01	<0.01	0.01	0.01	0.01	0.01	-	0.01	-
Fe^{2+}	5.35	5.23	5.31	5.49	5.78	4.57	4.99	0.81	1.07	2.43	4.92	2.76
Mn	0.03	0.03	0.03	0.03	0.03	0.03	0.04	0.02	0.02	0.03	0.02	0.01
Mg	3.27	3.42	3.38	3.96	3.75	4.29	4.08	8.73	8.67	6.56	4.13	2.50
Ca	0.12	0.11	0.11	0.07	0.07	0.07	0.07	0.07	-	0.08	0.07	0.09
Na	0.01	0.01	0.01	-	0.02	-	-	0.02	0.03	0.02	-	0.11
K	-	-	-	-	-	-	-	-	-	-	-	1.47
Fe^{2+}/R^{2+}†	0.61	0.59	0.60	0.58	0.60	0.51	0.54	0.08	0.11	0.27	0.54	0.52

* Total iron as FeO

† $R^{2+} = Ca + Mg + Mn + Fe^{2+}$

24,25,26 Diabanites, coarse-grained rodingite with prehnite-pectolite veins, 24705

27,28,29,30 Diabanites, coarse-grained rodingite, 23443

31,32 Penninites, chloritized serpentinite, 24703

33 Diabanites, fine-grained rodingite, 23438

34 Ripidolite, vein rodingite, 24714

35 Biotite, hornblende gabbro, 24720

TABLE IV. Representative electron microprobe analyses of garnets from rodingites, Wairere Serpentinite.

	36	37	38	39	40	41	42
SiO_2	30.1	28.8	29.2	34.8	34.9	36.1	34.6
TiO_2	-	-	-	0.03	0.03	0.06	0.02
Al_2O_3	24.8	23.1	22.2	23.7	24.1	6.97	5.92
FeO*	0.86	2.38	3.97	1.49	1.04	20.9	23.2
MnO	-	0.03	0.08	0.02	0.02	0.07	0.02
MgO	0.08	1.54	0.20	0.09	0.11	0.12	0.10
CaO	37.6	37.2	35.8	35.1	38.4	34.6	34.6
Na_2O	0.22	0.07	0.19	0.05	0.15	0.06	0.04
K_2O	0.02	-	0.02	-	-	0.02	0.01
Total	93.68	93.12	91.66	95.28	98.75	98.90	98.51
†	10.31	10.09	10.17	11.10	11.14	12	12
Si	2.13	2.04	2.12	2.57	2.51	3.11	3.04
Al	2.07	1.93	1.90	2.06	2.04	0.71	0.61
Fe^3	-	0.08	0.10	-	-	1.29	1.39
Fe^2	0.05	0.07	0.14	0.09	0.06	0.21	0.32
Mn	-	-	0.01	-	-	0.01	-
Mg	0.01	0.16	0.02	0.01	0.01	0.02	0.01
Ca	2.86	2.82	2.70	2.77	2.95	3.19	3.26
Na	0.03	0.01	0.03	0.01	0.02	0.01	0.01

36,37 Hydrogrossulars,hornblende rodingite vein, 24725

38 " coarse-grained rodingite, 24703

39,40 " " " " , 23443

41,42 Andradite-grossulars, pyroxene rodingite vein, 24723

* Total iron as FeO

† Structural formulae recalculated on number of oxygen atoms indicated so as to allow for the substitution $Si^{4+} \rightleftharpoons 4H^+$ and with Fe^{2+}/Fe^{3+} adjusted so as to make $\Sigma Y = 2.000$, where possible. (Leach and Rodgers, in prep c).

Pyroxene-bearing rodingite veins Numerous greenish-grey rodingite veins, 6-8 cm wide, were found throughout the quarry cutting through blocky, mesh-textured serpentinite. All show a panidiomorphic-granular texture with large euhedral diallage and medium-grained euhedral, colourless diopside set in a matrix of fine-grained brown garnet and colourless to orange-tinted chlorite. An assymetric, compositional layering (24723) exists parallel to the contact due to the presence of either diallage or diopside; while the overall grain size and the amount of impurities in the garnet decrease towards the contact. Diallage is absent 4 cm from the contact and the diopside decreases in size and quantity. Two centimetres from the contact diopside disappears leaving a dark-brown garnet, poikilitically enclosing chlorite, alternating with layers of chlorite enclosing garnet.

A 2 mm zone of recrystallised serpentinite exists immediately adjacent to the vein and in 24724 rare flakes of pinkish pleochroic phlogopite occur within the serpentine and around a small extension of the vein. In places the mica is partially replaced by a yellow-green chlorite.

Hornblende-bearing rodingite veins were occasionally found, cutting unsheared, blocky serpentinite. These are mantled by hard white hydrogarnet zones. The hornblende rodingite (24725) consists of coarse to medium-grained, euhedral to subhedral crystals of green hornblende in a matrix of orange-brown prehnite. The hornblende is pleochroic in green, blue-green and brownish-green, exhibiting simple twinning on (010) and multiple twins on (110). Locally it poikilitically encloses chlorite and garnet blebs and larger crystals may be chloritised. Near the centre of the vein, plagioclase laths have been completely prehnitized and then garnetized around grain boundaries. Prehnite and chrysotile veins cut the rodingite perpendicular to the contact.

The rodingite veins are bounded by a 1-2 cm wide hydrogarnet (hischite) zone. The hibschite is brown in thin section enclosing parallel, aligned chlorite specks. This zone is, in turn, separated from the host serpentinite by a further zone of 2-5 mm euhedral orthopyroxenes. A thin zone of coarse-grained euhedral, colourless clinopyroxene, twinned about (110), occurs in places along the contact between the hydrogarnet zone and the rodingite vein. In 24699, two hibschite zones are present, being separated by 7 mm of rodingite. Hornblende grains are sometimes continuous across the contacts of both these zones. Elsewhere, 3-4 cm wide hydrogarnet veins (23434) branch off from the hibschite zones and cut through blocky mesh-textured serpentinite.

Relic harzburgite pods

The highly sheared serpentinite contains small pods of blocky serpentinite that are almost completely serpentinised apart from some relic peridotite minerals. The most abundant relic mineral is orthopyroxene. Primary clinopyroxene and olivine is much rarer. Scattered chrome-spinels show the least alteration but generally exhibit tensional fracturing. Although it is impossible to estimate the modal proportions of these minerals in the original ultramafic rock it is clear that the Wairere Serpentinite was a harzburgite prior to alteration (cf O'Brien and Rodgers, 1974).

TABLE V Representative electron microprobe analyses and structural formulae of feldspar, pectolite, titanite and chrome spinel, Wairere Serpentinite

	43	44	45	46	47	48	49	50	51	52	53
SiO_2	65.7	65.5	57.7	48.1	53.3	54.6	30.6	31.0	30.4	0.41	0.20
TiO_2	0.01	0.02	0.01	0.07	-	-	35.9	35.7	35.3	0.04	0.15
Al_2O_3	19.7	19.4	27.0	31.6	0.05	0.05	1.50	1.87	1.82	24.7	34.0
Cr_2O_3	-	-	-	-	-	-	-	-	-	40.8	35.1
FeO*	0.07	0.13	0.12	0.47	0.24	0.21	0.51	0.51	0.17	20.2	17.5
MnO	-	-	-	-	-	-	-	-	-	0.40	0.31
MgO	0.08	0.06	0.07	0.16	0.06	0.06	0.02	0.02	0.02	13.0	12.8
CaO	1.52	1.97	5.41	14.8	32.6	33.2	31.0	31.0	31.0	0.04	0.01
Na_2O	11.1	10.8	7.17	3.36	8.53	8.80	0.06	0.06	0.03	0.05	0.04
K_2O	0.16	0.27	0.10	0.19	0.02	0.08	-	0.01	-	0.01	0.01
Total	98.34	98.15	97.58	98.75	94.80	97.00	99.59	100.17	98.74	99.65	100.12
Si †	11.75	11.76	10.48	8.95	6.03	6.04	1.01	1.02	1.01	0.10	0.05
Ti	-	< 0.01	-	0.01	-	-	0.89	0.88	0.88	0.01	0.03
Al	4.15	4.10	5.78	6.93	0.01	0.01	0.06	0.07	0.07	7.32	9.54
Cr	-	-	-	-	-	-	-	-	-	7.72	6.29
Fe^{2+}	0.01	0.02	0.02	0.07	0.02	0.02	0.01	0.01	0.005	4.25	3.49
Mn	-	-	-	-	-	-	-	-	-	0.09	0.06
Mg	0.02	0.02	0.02	0.04	0.01	0.01	-	-	-	4.87	4.54
Ca	0.29	0.38	1.05	2.95	3.95	3.93	1.10	1.09	1.10	0.01	-
Na	3.85	3.76	2.53	1.21	1.87	1.89	<0.01	<0.01	<0.01	0.02	0.02
K	0.04	0.06	0.02	0.05	-	0.01	-	-	-	-	-

43,44 Plagioclases, altered eucritic gabbro, 23448
45,46 Rim and core, respectively, of plagioclase, hornblende gabbro, 24720
47 Pectolite, pectolite-prehnite zone, 24705
48 Pectolite, vein in altered gabbro, 23448
49,50 Titanite, unaltered hornblende gabbro, 24720
51 Titanite, chlorite vein, 24714
52 Chrome-spinel, relic in serpentinized harzburgite, 23449
53 Chrome-spinel, relic in sheared serpentinite adjacent to pyroxene-rodingite vein, 24723

† Structural formulae calculated on a basis of 32 oxygen (feldspar), 17 oxygen (pectolite), 5 oxygen (titanite) and 32 oxygen (chrome-spinel).

TABLE VI. Analyses of rodingites, gabbros and associated rocks from Wairere, New Zealand

	1	2	3	4	5	6	7	8	9	10	11	12	13	14	15	16	17	18
SiO_2	44.4	41.7	41.6	36.4	40.5	33.5	37.1	34.6	36.6	34.5	50.3	43.0	33.0	38.6	40.2	39.4	1.7	1.4
TiO_2	2.6	1.7	2.6	2.6	1.7	1.2	2.1	2.2	1.9	2.1	0.1	1.2	1.3	0.2	-	-	-	-
Al_2O_3	14.6	15.0	14.8	15.0	12.8	16.7	13.1	16.5	11.9	15.2	14.9	12.3	15.9	4.2	1.0	-	3.2	2.0
Fe_2O_3	0.2	2.0	1.0	0.6	1.2	2.1	2.6	1.7	2.4	5.5	3.8	4.2	3.9	3.2	2.6	5.9	-	-
FeO	9.4	7.2	8.0	10.0	6.9	7.3	5.9	5.9	5.5	6.5	5.8	3.9	4.0	3.5	1.7	1.9	0.1	0.1
MnO	0.15	0.15	0.15	0.18	0.1	0.18	0.1	0.2	0.15	0.24	0.18	0.18	0.18	0.11	0.05	0.07	-	-
MgO	4.3	5.1	4.8	8.3	5.5	7.1	5.4	8.0	6.3	7.7	6.9	5.0	10.8	35.1	38.0	36.6	0.3	0.3
CaO	16.4	20.0	19.7	22.2	24.7	25.0	27.3	23.0	28.4	21.1	14.2	22.2	20.3	1.2	1.7	3.2	52.8	53.5
Na_2O	2.5	1.6	1.9	0.25	1.6	0.6	0.6	0.6	0.15	0.4	0.1	2.7	2.5	0.15	0.1	0.1	0.26	0.26
K_2O	0.6	0.03	0.9	-	0.2	0.03	0.03	0.05	tr	0.03	0.18	tr	0.02	0.03	-	-	0.03	0.03
P_2O_5	0.05	0.07	0.1	0.03	0.02	0.03	0.03	0.03	0.13	0.13	0.16	0.17	0.19	0.03	0.3	-	0.13	0.07
CO_2	-	0.8	0.3	-	0.6	-	0.4	-	0.3	-	-	-	-	-	0.55	-	41.7	42.1
H_2O+	4.5	4.5	4.0	4.3	4.0	6.0	5.1	6.8	6.0	6.2	3.2	4.6	8.0	13.3	13.6	12.6	<0.1	<0.1
Total	99.70	99.85	99.85	99.86	99.82	99.74	99.76	99.58	99.73	99.60	99.82	99.45	100.9	99.62	99.80	99.77	100.22	99.76

1 Altered gabbro, 23447, centre pod B
2 Altered gabbro, 23448, centre pod C
3 Coarse-grained rodingite, 23444, 20 cm from contact, pod B
4 Coarse-grained rodingite, 23443, at contact, pod B
5 Coarse-grained rodingite, 23442, 20 cm from contact pod C
6 Coarse-grained rodingite, 23437, at contact, pod C
7 Fine-grained rodingite, 23436, 20 cm from contact, pod B
8 Fine-grained rodingite, 23435, at contact, pod B
9 Fine-grained rodingite, 23439, 20 cm from contact, pod C
10 Fine-grained rodingite, 23438, at contact, pod C
11 Unaltered hornblende gabbro, 24720
12 Altered hornblende gabbro, 24712
13 Rodingite at hornblende gabbro contact, 24713
14 chloritised serpentinite, 23440, at pod contact
15 Chloritised serpentinite, 23441, 20 cm from pod contact
16 Massive serpentinite after harzburgite, 23449
17 Otorohanga limestone, 23445, at serpentinite contact
18 Otorohanga limestone, 23446, 40 m from serpentinite contact

For pod descriptions and sample number locations see Leach and Rodgers (in prep b). Analyst: T H Wilson

Summary

The mafic inclusions within the Wairere Serpentinite exhibit a wide variety and degree of metasomatism. Initial alteration has albitized the plagioclase, followed by conversion to prehnite or clinozoisite. Original mafic minerals, clinopyroxene and hornblende have been altered to chlorite. More intense metasomatism of the gabbros has garnetized the prehnite (to hydrogarnet) and has generated secondary clinopyroxene and hornblende. Adjacent to the contacts, the hydrogarnet content of the rodingite increases and is possibly the end product of rodingitization. The original harzburgite has been highly serpentinized and, at the contact with most gabbroic inclusions, the serpentine has been altered to a blue-green chlorite zone.

The borders of the gabbros exhibit cataclasis and brecciation, indicating strong tectonic movements before being emplaced in their present location. The rodingites show signs of more than one episode of metasomatism and this is possibly related to the tectonic history of the mafic-ultramafic assemblage.

Acknowledgements Much of the equipment used in this study was provided by various grants of the New Zealand University Grants Committee and the Auckland University Research Grants Committee. Thanks are due to Mr Rorrison and Mr Taylor of the Wairere serpentine quarry for their considerable assistance and to Dr P M Black whose suggestions considerably improved the manuscript.

References

O'Brien (J.P.) and Rodgers (K.A.), 1973a. *Journ.Roy.Soc.N.Z. 3*, 169-90.

________________, 1973b. *Mineral.Mag. 39*, 233-40.

________________, 1974. *Journ.Roy.Soc.N.Z. 4*, 141-60.